Protein Attraction in Membranes Induced by Lipid Fluctuations

T. Sintes and A. Baumgärtner
Forum Modellierung, Forschungszentrum, 52425 Jülich, Germany

ABSTRACT The nonspecific lipid-mediated attraction between two proteins embedded in a bilayer membrane have been investigated for a model system using Monte Carlo simulations. We found two types of attraction with different regimes. A depletion-induced attraction in the range $r < \sigma_L$, where σ_L is the diameter of a lipid and r is the distance between the surfaces of the two proteins, and a fluctuation-induced attraction in the range $1 < r/\sigma_L < 6$, which originates from the gradients of density and orientational fluctuations of the lipids around each protein. The effective potential of the latter type of attraction decays exponentially with $U(r) \sim \exp(r/\xi)$ where the correlation length is $\xi/\sigma_L \approx 3.2$ in the present model system.

INTRODUCTION

Biological membranes are highly heterogeneous. They may consist of mixtures of different lipids and a variety of different proteins. Many of the proteins are mobile and may aggregate and form clusters, pores, and channels that are important for cellular processes. Therefore the origins of forces responsible for aggregation is of basic importance for our understanding of formation of membrane protein aggregates.

The process of aggregation can be quite complex and may be attributed to several mechanisms (Lemmon and Engelman, 1994). Aggregation can be initiated by specific intermolecular forces (Israelachvili, 1992) encountered, for example, at temperature-driven phase separations among lipids and proteins (Mouritsen and Bloom, 1993), or by electrostatic attraction between dipoles on pairs of antiparallel α-helices (Ben-Tal and Honig, 1996). Another situation is concerned with asymmetric properties of curved membranes and asymmetric shapes of embedded proteins, which both may induce aggregation of proteins (Odell and Oster, 1994). A third class of aggregation mechanism is related to long-range membrane-mediated attraction between two inclusions (Gruler and Sackmann, 1977; Goulian et al., 1993; Bruinsma et al., 1994; Aranda-Espinoza et al., 1996). This force is due to the correlation between the perturbations imposed by the inclusions on the membrane's long-range undulations.

In addition to the undulation-mediated attraction, it has been argued that at short distances, in the order of a few lipid layers between two proteins, a nonspecific lipid-mediated attraction may exist (Marcelja, 1976; Schröder, 1977; Owicki and McConnell, 1979; Pearson et al., 1984). This short-range interaction may be important for the stabilization of tight clusters of inclusions encountered, e.g., during the aggregation of pore forming membrane helices. In the Marcelja model the lipid-protein interactions are described by the average perturbation of the orientational order parameter of the lipids $S(r)$ around a protein represented by a hard cylinder. The important result of this approach is the prediction of an effective attraction between cylinders when the order parameter profiles of neighboring proteins overlap leading to a decrease of the total perturbation of the lipid structure.

In the present article we report on a detailed investigation of lipid-mediated attraction between two inclusions. By using Monte Carlo simulations of two cylindrical inclusions approximating two α-helices or two proteins embedded in a lipid bilayer membrane, we have estimated the forces between the inclusions and the range of attraction. It is shown that there exist two types of lipid-mediated attractive forces. The first type of force, which we call the Asukara-Oosawa attraction, is limited to a lipid depletion zone around the proteins and hence is of short range, about $r < \sigma_L$ where σ_L is the thickness of a lipid molecule. The second type of attractive force, which is dominated by the first type at very short distances, is induced by the density fluctuations and the orientational fluctuations of the lipids around a protein. Although the range of this fluctuation-induced attraction seems to decay exponentially, the observed effective range of attraction is rather large and in the order of $1.5 < r/\sigma_L < 6$ in our simulations.

MODEL MEMBRANE AND SIMULATION TECHNIQUE

The lipid bilayer

We have simulated a lipid bilayer at air-water interface using Monte Carlo methods. We have considered an assembly of $N_L = 2 \times 500$ lipid molecules and two cylinders ("proteins") confined in a unit box with periodic boundary conditions in the $x - y$ domain. Initially the length of the cell is chosen to be at least 10 times the diameter of the protein to make finite size effects negligible. Proteins are represented by hard cylinders of diameter σ_P, whose axes are located perpendicularly to the $x - y$ plane. We have modeled a lipid molecule by a flexible chain of $M = 5$

Received for publication 29 April 1997 and in final form 4 August 1997.
Address reprint requests to Dr. Artur Baumgärtner, Forschungszentrum, D-52425 Julich, Germany. Tel.: 49-2461-61-4074; Fax: 49-2461-61-2620; E-mail: a.baumgaertner@kfa-julich.de.

0006-3495/97/11/2251/09 $2.00

effective monomers of diameter $\sigma_L = 4$ Å. Each monomer represents a group of ~3–4 successive chemical monomers (CH_2 groups) of a real lipid molecule (Haas et al., 1995). Within this coarse-grained model, the distribution of the angle between subsequent effective bonds can be modeled by a suitable effective potential for bond angles, and the correct persistence length of the chains can be, at least, reproduced roughly. Thus, effective intramolecular potentials are introduced to take into account chain connectivity and chain stiffness. Because of these coarse-graining along the chain we do not consider any torsional potential.

The total energy of the lipids contains the following contributions:

$$U = U_{bond} + U_{angle} + U_{steric}. \quad (1)$$

Commonly used potentials and parameters for U have been taken from previous Monte Carlo simulations (Xiang, 1993; Baumgärtner, 1995). The vibrational energy of the bonds along the chain backbone is

$$U_{bond} = \sum_{bond} \epsilon_b (b/b_0 - 1)^2, \quad (2)$$

where $\epsilon_b = 250$ kcal/mol and $b_0 = 3.9$ Å. We use an upper and lower bond for the extension of the spring such that $U_{bond}(b > b_{max}) = U_{bond}(b < b_{min}) = \infty$, where $b_{min} = 3.6$ Å, $b_{max} = 4.2$ Å. The bending energy between neighboring bonds is

$$U_{angles} = \sum_{angles} \epsilon_\theta (1 + \cos\theta)^2, \quad (3)$$

where $\epsilon_\theta = 15$ kcal/mol. The last term represents the steric interactions among the monomers of the lipids,

$$U_{steric} = \sum_{i,j=1}^{M \times N_L} V(r_{ij}), \quad (4)$$

where V is a hard sphere potential

$$V(r_{ij}) = \begin{cases} 0, & \text{for } |\mathbf{r}_i - \mathbf{r}_j| > \sigma \\ \infty, & \text{for } |\mathbf{r}_i - \mathbf{r}_j| < \sigma \end{cases} \quad (5)$$

and $\sigma = \sigma_L$ was employed for intermolecular interactions and for interactions between monomers that are separated by more than one bond in the same molecule. Similarly, the steric interactions between the monomers of the lipids and the proteins have been taken into account by the same hard core potential, but then $\sigma = (\sigma_P + \sigma_L)/2$.

Since in our model system the specific interactions between water and lipids and among the lipid heads are not included, we have to use a mechanism providing the stability of the bilayer structure of our model membrane. Stability with respect to perpendicular deviations from the two-dimensional structure can be provided by designing fixed interfaces separating the lipid head groups and the hypothetical aqueous environment, and by tethering the head groups to these artificial interfaces. The two interfaces for the upper and lower leaflets of the bilayer membrane are modeled by two impenetrable and flat surface at $z = 40$ Å and $z = 0$ Å for the upper and lower interfaces, respectively. The lipid heads of the upper and lower leaflets are tethered to their corresponding interfaces. Each tether is modeled for simplicity by an athermal potential $U(z)$, where $U(z) = 0$ for $0 < z < \sigma_L$ and $40 > z > (40 - \sigma_L)$, and $U(z) = \infty$ otherwise. The separation of 40 Å between the two interfaces has been chosen with regard to usual experimental situations and with regard to minimize the steric repulsion between the two leaflets of the bilayer. By construction the lipids are bound by their heads to their interfaces, but are otherwise free to perform Brownian motions and to diffuse in the $x - y$ plane. The stability of our model membrane with respect to extensions in the $x - y$ plane is achieved by imposing periodic boundary conditions on the basic cell as defined above. A snapshot of the lipid bilayer is depicted in Fig. 1.

Simulation details

To simulate the model we employed the Metropolis Monte Carlo algorithm. A molecule, lipid, or protein is randomly selected at each trial move. If a protein is selected, a displacement of the cylinder parallel to the $x - y$ plane in a randomly chosen direction is attempted. The dynamics of the lipids are achieved by randomly displacing their constituents. Each move is accepted if

$$\exp(-\Delta U/RT) > \eta, \quad (6)$$

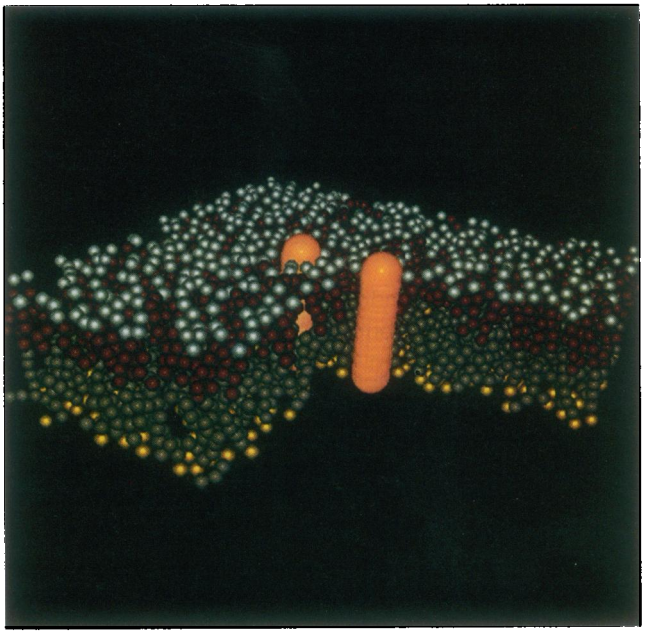

FIGURE 1 Snapshot of the bilayer and its two inclusions. Each of the spheres, which are the subunits of the lipid chain molecules, has a diameter of 4 Å. Diameter and length of a cylindrical inclusion are 16 and 40 Å, respectively. For the sake of clarity we have removed a portion of the bilayer.

where $0 < \eta < 1$ is a random number, ΔU is the difference between the old and the new energy of the system. Throughout the simulations we used a temperature of $T = 305$ K and hence $RT = 0.606$ kcal/mol. One Monte Carlo Step (MCS) corresponds in the case of N_L lipids and two inclusions to $M \times N_L + 2$ attempted moves and is defined as one time unit. The maximum distance translated by the particles is adjusted to optimize the acceptance rate. A link-cell method (Allen and Tildesley, 1987) has been implemented in the algorithm to efficiently check ΔU.

Each particular simulation starts by placing the centers of the two cylinders at a distance $r = \sigma_P + \delta r$. The initial locations and orientations of the lipids are at random. The system has been relaxed at a constant pressure of 70 dyn/cm. The isobaric equilibration is performed by allowing the length of the system L in the $x - y$ plane to vary. An attempt to rescale the system area, and thus the position of all the particles, is performed every 10 MCS and is accepted according to the energy condition (6) and a Boltzmann factor (Allen and Tildesley, 1987),

$$\exp\left[-\beta P \Delta A + N_L \log\left(1 + \frac{\Delta A}{A}\right)\right] \tag{7}$$

where P is the pressure and ΔA is the difference in the area ($A = L^2$) before and after the rescaling. The equilibration process needs $\sim 10^5$ MCS (during this time the proteins are immobile). The final area depends slightly on the diameter of the proteins. We have considered proteins with σ_P ranging from 8 Å to 16 Å. The mean area per lipid, after the equilibration process, is ~ 48 Å^2. The average orientation of the lipids respect to the normal surface is $\langle \cos(\theta) \rangle = 0.81$. Both, the average tilt angle and area per lipid are comparable to experimental values (Gennis, 1989). In Fig. 1 we present a snapshot of the lipid bilayer for $\sigma_P = 16$ Å. The centers of the proteins are separated a distance $r = \sigma_P$ (that is, their surfaces are $4\sigma_L$ apart).

Computing the forces

A method to estimate the average lipid-mediated force between two helices has been discussed recently (Sintes and Baumgärtner, 1997) and is related to a technique developed for a colloidal dispersion in a nonadsorbing polymer solution (Dickman and Yethiraj, 1994). The method is limited to *two-body* forces, which has to be distinguished from many-body effects (Meijer and Frenkel, 1994) as encountered, e.g., in lipid-protein mixture.

The basic idea is to relate the force to the local perturbation in the density field. One computes the change in the free energy F due to an infinitesimal change δr in the relative position of the inclusions. The force, in units of $k_B T$, is given by

$$f(r) \equiv \frac{F}{k_B T} = \frac{\partial \ln Z(r)}{\partial r}, \tag{8}$$

where $Z(r)$ is the partition function of the system which is the set of allowed configurations of the lipids in the presence of the inclusions; $f(r) > 0$ corresponds to a repulsive force directed along the line joining the cylinders.

Consider a system with two cylindrical inclusions at a fixed distance r. Let $\Omega_C(r) \subset Z(r)$ be the configurations that are allowed when one of the inclusions is shifted toward the other one by a distance δr without violating the excluded volume condition between lipids and cylinders. Similarly, let $\Omega_E(r - \delta r) \subset Z(r - \delta r)$ be the set of configurations of $Z(r - \delta r)$ in which it is possible to shift the inclusions a distance δr apart without overlapping a lipid. The probability of bringing an inclusion closer is just $P_C(r) = \Omega_C(r)/Z(r)$, and the probability that the inclusions may be shifted from a distance $r - \delta r$ to r is $P_E(r - \delta r) = \Omega_E(r - \delta r)/Z(r - \delta r)$. Since the subsets $\Omega_C(r)$ and $\Omega_E(r - \delta r)$ are in one to one correspondence, we have

$$\frac{Z(r)}{Z(r - \delta r)} = \frac{P_E(r - \delta r)}{P_C(r)}. \tag{9}$$

Because of the finite size step δr used in computer simulations, we approximate

$$\frac{\partial \ln Z(r)}{\partial r} \approx \frac{1}{\delta r} \ln \frac{Z(r)}{Z(r - \delta r)}. \tag{10}$$

We can take the mean with the expression corresponding to $r' = r + \delta r$. By using Eq. (9) the force is given by:

$$f(r) = \frac{1}{2\delta r} \ln\left(\frac{P_E(r - \delta r)}{P_C(r)} \frac{P_E(r)}{P_C(r + \delta r)}\right). \tag{11}$$

The probabilities P_C and P_E are determined by checking periodically whether moving the inclusions a distance δr closer or further apart would result in an overlap with a lipid.

The simulation procedure is as follows. Initially the proteins are separated at a distance $r = \sigma_P + \delta r$. Each particular study at a different σ_P value starts from the previously equilibrated configurations at a constant pressure ensemble. During this equilibration process, the cylinders remain immobile. At this point an attempt to shift the inclusion a distance δr closer or further apart is performed every 20 MCS. Notice that after the trial the protein remain in its original position. The probabilities $P_C(r)$ and $P_E(r)$ are evaluated after 10^3 collected data. Averages are taken over 50 different sets of data. The uncertainty is estimated by computing the standard deviation of the mean. Relaxation periods of 10^4 MCS are used between each change in r of the relative position of the inclusions. We have chosen in all our simulations $\delta r = 0.5$, and considered three different values of σ_P: 8, 12, and 16 Å.

RESULTS AND DISCUSSION

Properties of the model membrane

Before reporting on our results on the lipid-mediated interaction between inclusions, it is useful to characterize the

bulk and local properties of the unperturbed model membrane. The average tilt angle of the lipid chain molecules that we have defined as the average angle between the end-to-end vector $\mathbf{d} = \mathbf{r}_5 - \mathbf{r}_1$ of a lipid and the surface normal of the membrane is $\langle\cos(\theta)\rangle = 0.81$. The brackets $\langle \ldots \rangle$ denote thermal average.

Since in most experiments the molecular order parameter S_n is accessible, e.g., in deuterium NMR measurements on selectively deuterated compounds (see, e.g., Gennis, 1989), estimates of S_n from our simulations are presented in Fig. 2. The molecular order parameter

$$S_n = -S_{CD} \tag{12}$$

represents the orientation of the vector perpendicular to the plane formed by the CD_2 groups of the acyl chains, where S_{CD} is defined along the C–D bond (Egberts et al., 1994) by

$$S_{CD} = 2/3S_{xx} + 1/3S_{yy} \tag{13}$$

where the order parameter tensor is

$$S_{ij} = \frac{1}{2}\langle 3\cos\Theta_i\cos\Theta_j - \delta_{ij}\rangle \tag{14}$$

and Θ_i is the angle between the ith molecular axis and the bilayer normal. The brackets denote the ensemble average. Molecular axes are defined per CH_2 group. Although in the present coarse-grained model of lipid chain molecules the CH_2 groups are not specified, we have defined the local C–D bonds to be perpendicular to the plane formed by two successive segments along the chain molecule. The parabolic form of S_n is consistent with experimental facts (Gennis, 1989) and supports the appropriateness of the present model membrane.

For comparison we have included in Fig. 2 the average orientation of each segment n of the chain with respect to the plane of the membrane,

$$S_z(n) = \frac{1}{2}\langle 3[z_{n+1} - z_n)/a_n]^2 - 1\rangle, \tag{15}$$

where $\mathbf{a}_n = \mathbf{r}_{n+1} - \mathbf{r}_n$ and $z_{n+1} - z_n$ are the segmental vector and its z-component, respectively. The results are comparable to the molecular order parameter S_n.

Another interesting quantity characterizing the lipid molecules is the stiffness of the chain. One possibility to define the local chain stiffness is the average angle between the segmental vector $\mathbf{a}_n$ and the end-to-end vector $\mathbf{d}$. The results for the local stiffness $S_d(n) = \frac{1}{2}\langle 3[\mathbf{d}\cdot\mathbf{a}_n/da_n]^2 - 1\rangle$ are presented in Fig. 2. As expected the local stiffness is lower at the ends of the chain and essentially independent of head or tail.

The density profile of the bilayer membrane $\rho(z) = \Sigma_j\langle z_j\rangle$, where the index j runs over all five N_L monomers of the lipid bilayer, is presented in Fig. 3. The oscillatory shape reflects the stiffness of the lipid chains.

The force between two proteins

We have determined the lipid-mediated force between the cylindrical inclusions using the Monte Carlo techniques as described above. The data are presented in Fig. 4.

The short-range part of $f(r)$ for $r/\sigma_L < 1$ can be understood based on the two-dimensional version of the Asakura-Oosawa approach (Asakura and Oosawa, 1958). The force between two cylinders suspended in the solution of lipids is

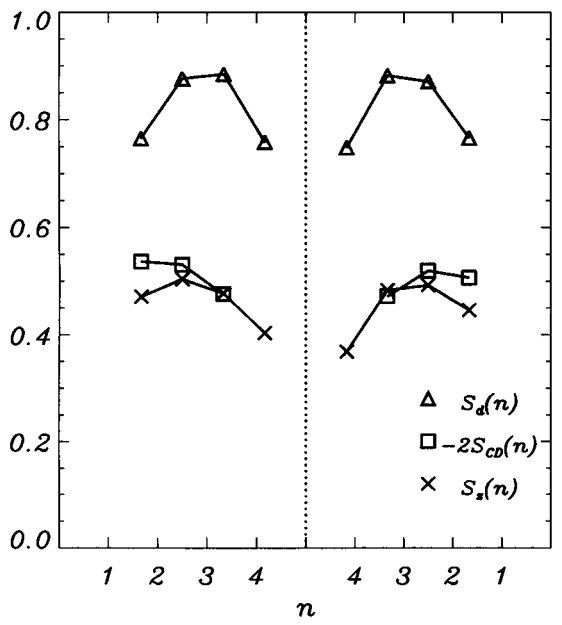

FIGURE 2 Segmental chain stiffness $S_d(n)$ segmental chain orientation $S_z(n)$, and molecular order parameter S_n for each segment n of the lipid chain molecule.

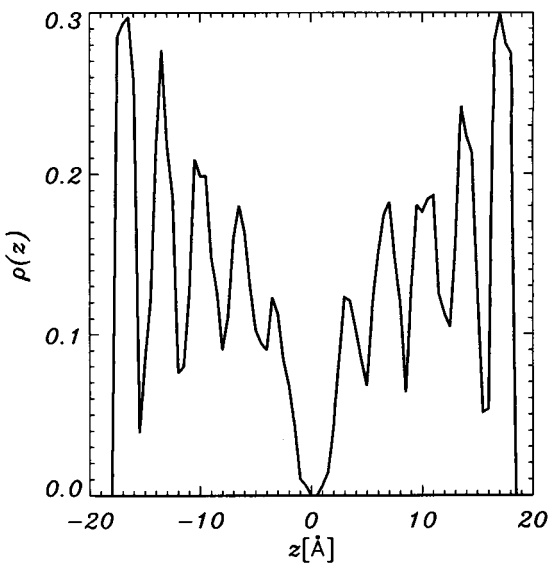

FIGURE 3 Density profile $\rho(z)$ of the lipid bilayer.

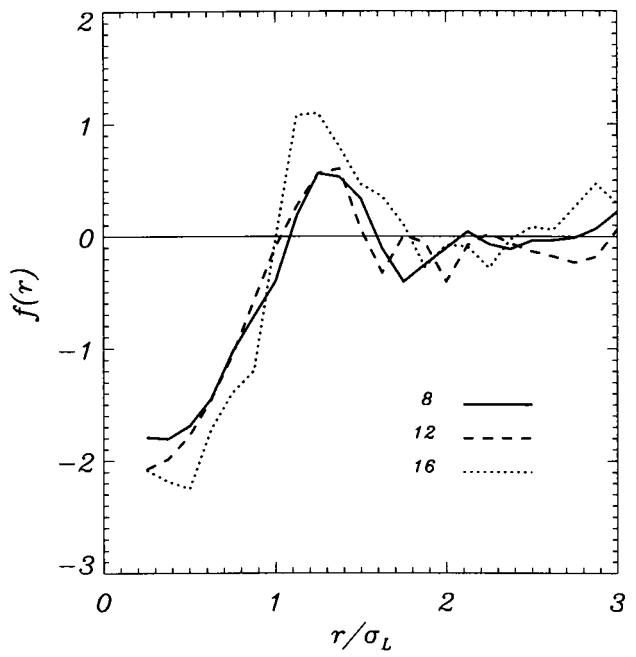

FIGURE 4 Force $f(r)$ versus distance r/σ_L for various diameters σ_P of cylinders.

given by

$$f(r) = N_L \frac{\partial \ln Q}{\partial r} \tag{16}$$

$$Q = \int_V \exp[-U(\mathbf{r}, r)/k_B T]d\mathbf{r} \tag{17}$$

where $U(\mathbf{r}, r)$ is the interaction energy of a lipid located at $\mathbf{r}$ in the presence of the two cylinders separated by a distance r. A negative value of $f(r)$ corresponds to attraction between the cylinders. Since the interaction energy is purely repulsive, Q is given by the area of space in which the lipids can move freely. One obtains Q by subtracting from the total area of the solution the area into which the lipids cannot enter due to hindrance of the cylinders, which is given by

$$Q = A - 2A_0 + 2S, \quad r/\sigma_L < 1 \tag{18}$$

where $A_0 = \pi(\sigma_L + \sigma_P)^2/4$ is the area including one cylinder and its depletion area of width σ_L, and S is the corresponding cross-sectional area of the two overlapping effective cylinders, each having an area of A_0. The cross-sectional area is given approximately by

$$S = z^{3/2}\left(\frac{4}{5}\sqrt{\sigma - z^{3/2}} + 8\sqrt{\sigma/2}\right) \tag{19}$$

where

$$z = \frac{\sigma_L}{2}\left(1 - \frac{r}{\sigma_L}\right) \tag{20}$$

and $\sigma = \sigma_L + \sigma_P$. The derivative $\partial Q/\partial r$ has the limiting cases

$$\frac{\partial Q}{\partial r} \sim -\sqrt{1 - r/\sigma_L}, \quad \text{for } r/\sigma_L \to 1 \tag{21}$$

and

$$\frac{\partial Q}{\partial r} \sim c_1 r/\sigma_L - c_2, \quad \text{for } r/\sigma_L \to 0, \tag{22}$$

where c_1, c_2 are some positive constants. In Fig. 5 we have plotted $f(r)/k_B T$ in the regime $r/\sigma_L < 1$ according to Eq. 16 and the corresponding Monte Carlo data. The qualitative agreement between Monte Carlo data and the simple theory is quite remarkable, although the crossover to $r/\sigma_L \to 0$ indicates some systematic deviations. It is conceivable that in this limit the proximity of the second minimum around $r/\sigma_L \approx 2$ affects the data close to $r/\sigma_L = 1$, and hence the theory cannot be expected to be in perfect agreement with our data. With regard to the fact that depletion-induced attraction has been measured in recent experiments on colloid-polymer mixtures (Ohshima et al., 1997), it is not unrealistic to expect such effects for proteins in membranes as well, similar to those observed in our simulations.

According to Fig. 4 this regime of depletion-induced attraction is separated from a second regime of protein-protein attraction at larger distances (as discussed below) by a repulsive barrier in the range $\sim 1 < r/\sigma_L < 1.5$. The repulsion is a result of chain packing and can be understood as follows. At protein-protein distances slightly larger than the depletion regime some lipids may interfere between the two proteins. The according distance must be larger than the

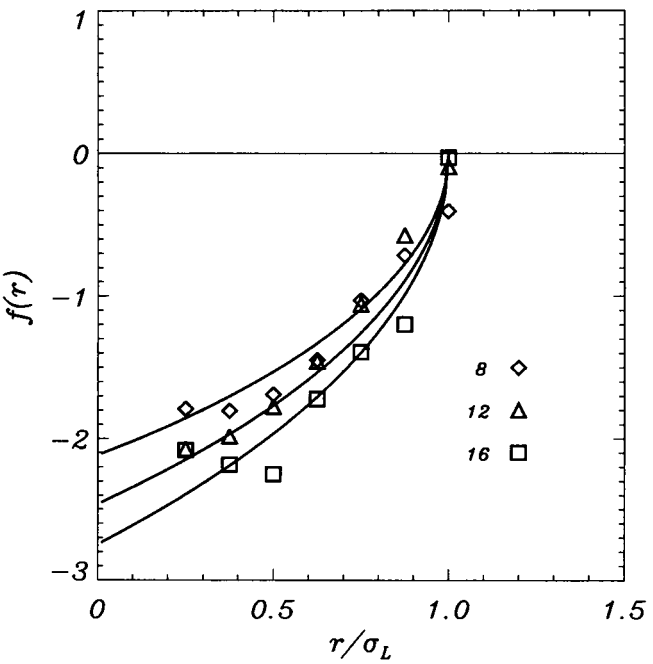

FIGURE 5 Comparison between theory, Eqs. 16–20, and Monte Carlo data for $f(r)$ in the range $r/\sigma_L < 1$.

diameter of one lipid in order to accommodate the average orientational and translational entropy of the lipids of the bulk. Since the average distance between the lipids in the bulk is $\sim r/\sigma_L \approx 1.7$, any distance between the proteins smaller than this would result in a repulsion between them.

Beyond this repulsive regime, $r/\sigma_L > 1.5$, the force again becomes attractive. According to the estimates $f(r) < 0$ (Fig. 4), the standard deviation of the data points is <10% and of the order of the thickness of the lines. However, from the sampling method used in determining the forces from the measured probabilities, one can expect larger error bars. In fact, after the second minimum the curves are at the level of sensitivity of the method and it is difficult to determine their behavior and range. We expect such interaction to be more important than the thermal fluctuations introduced through the Boltzmann factor; therefore we have examined in detail the perturbations of the density of lipids and their orientational order in the vicinity of the proteins in order to characterize the long-range attractive interaction.

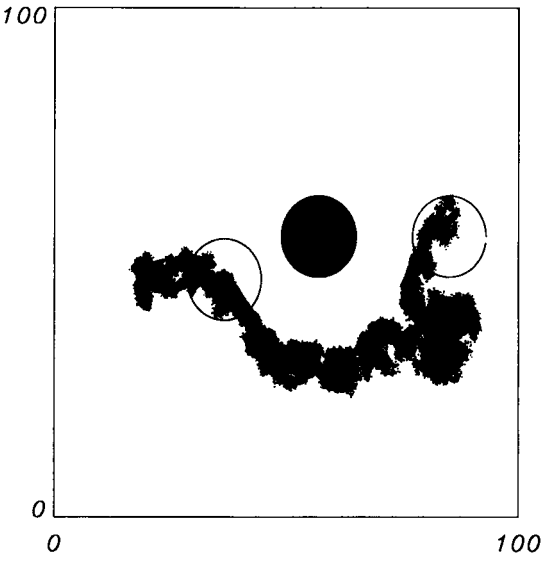

FIGURE 6 Diffusion of one mobile protein in the vicinity of a second immobile protein. The location of the immobile protein and the initial location of the mobile protein are represented by circles of diameter 16 Å. Each dot represents the center of the mobile protein at different times.

Fluctuation-induced attraction between proteins

In the following paragraph we provide some evidence for a nonspecific fluctuation-induced protein-protein attraction beyond the repulsive barrier at distances $r/\sigma_L > 1.5$.

The simplest way to demonstrate the existence of a net attractive force between the proteins is to monitor the time-dependent positions of one mobile protein with respect to a second, but immobile, protein. If the mobile protein is attracted by the immobile one, then the diffusional path of the mobile protein must exhibit approximately a circular trajectory around the immobile protein in the $x - y$ plane. Otherwise, in the case of vanishing attraction, the mobile protein would perform a random walk with the tendency to escape from the vicinity of the immobile protein.

The result of this simulation is shown in Fig. 6. The mobile protein was initially placed outside the repulsive regime at $r/\sigma_L = 3$. In order to monitor exclusively the random motion in the regime $r/\sigma_L > 1.5$, we had to prevent the transition of the mobile protein into the depletion zone $r/\sigma_L < 1$ of the immobile protein. Therefore its motion had been restricted to $r/\sigma_L > 1$. Every dot in Fig. 6 represents the location of the center of the mobile protein at a different time and hence the total "cloud" represents the visited area. The total run took $\sim 10^7$ MCS that we consider to be long enough to be representative of the behavior of the system. Every 200th position is depicted in Fig. 6. The initial and final position of the mobile protein are denoted by open circles, the immobile protein is denoted by the filled circle.

Before discussing the consequences to be inferred from Fig. 6, we want to point out some remarks on the diffusion coefficient and the Monte Carlo time scale as compared to experiments. In order to compare the Monte Carlo time with experimental time scales it is reasonable to assume that a typical relaxation time of one of the monomers of the lipid molecule, which is in the order of $\tau \approx 10^{-9}$s, corresponds to one MCS. Since the mean squared displacement of the mobile protein is approximately $\langle r^2(t)\rangle = 1600$ Å^2 after $t = 10^7$ MCS, the resulting diffusion coefficient is calculated to $D = \langle r^2(t)\rangle/t\tau = 0.16 \times 10^6$ Å^2 s^{-1}. This is in reasonable agreement with experimental results where the typical diffusion constants for proteins and lipids are $D \approx 10^5$ Å^2 s^{-1} and $D \approx 10^8$ Å^2 s^{-1}, respectively (Peters, 1988).

The trajectory of the mobile protein as depicted in Fig. 6 clearly demonstrates the existence of an attractive force beyond the depletion and repulsive zones. The mobile protein performs a semicircular path around the immobile protein until we stopped the simulations. The corresponding probability distribution $P(r)$ of inter-protein distances is shown in Fig. 7. The maximum distance between the two proteins along the semicircular path is about $r_{max}/\sigma_L \approx 6$, which we define as the effective range of attractive interaction in the present model system.

It will be shown below that the origin of the attractive force is related to the gradients of density and orientational fluctuations of the lipids in the neighborhood of the proteins. This suggestion follows the predictions from mean-field calculations of Marcelja (1976) and Schröder (1977).

Figs. 8 and 9 show the average profiles of lipid orientational order and density and their corresponding fluctuations around a *single* protein. Accurate estimates of these quantities in the presence of two proteins, which would correspond to the situation depicted in Fig. 6, had been too difficult due to the radial anisotropy caused by the mutual perturbation of the two proteins upon each other.

In Fig. 8 we present the density profile of lipids around a single immobile protein

$$\rho(r) = \sum_j \theta(r - r_j) \Big/ \pi r^2 dr \qquad (23)$$

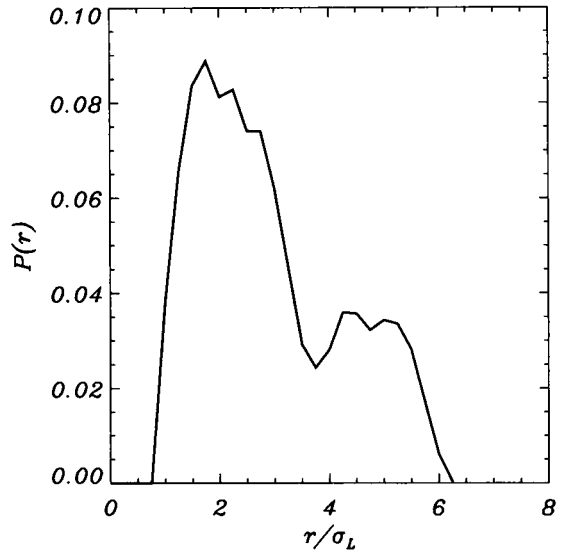

FIGURE 7 Probability distribution $P(r)$ of inter-protein distances.

where the sum runs over all monomers $1 \leq j \leq 5N_L$ located at distances $r_j = \sqrt{x_j^2 + y_j^2}$ with respect to the surface of a protein of diameter $\sigma_P/\sigma_L = 4$. The θ-function is defined as $\theta(r - r_j) = 1$ if $|r - r_j| < dr = 0.5$ Å and zero otherwise. For large distances $r/\sigma_L \gg 1$ one obtains the bulk value $\langle\rho(\infty)\rangle = 0.22$. At short distances $r/\sigma_L < 1$ the density decreases according to a depletion zone. Included in Fig. 8 is the lipid orientational profile

$$S(r) = \sum_j S_z(r_j)\theta(r - r_j) \Big/ \sum_j \theta(r - r_j) \qquad (24)$$

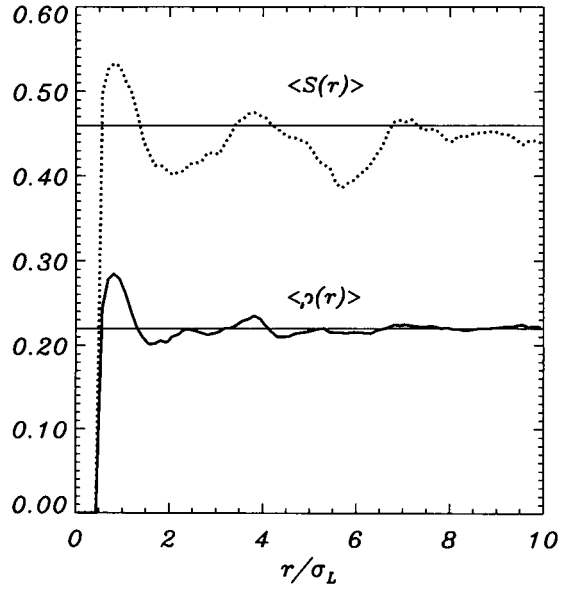

FIGURE 8 Density profile $\langle\rho(r)\rangle$ and orientation profile $\langle S(r)\rangle$ of lipid molecules around one protein.

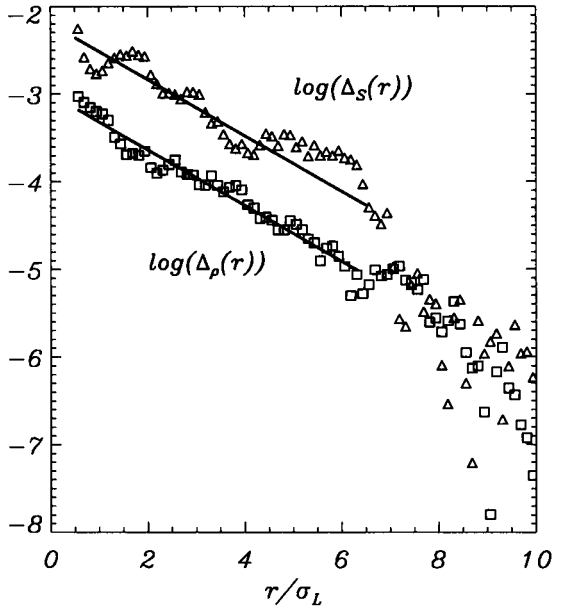

FIGURE 9 Semilog plot of the fluctuations $\Delta_\rho(r) = \delta\rho(r) - \delta\rho(\infty)$ and $\Delta_S(r) = \delta S(r) - \delta S(\infty)$.

where $S_z(r_j)$ is defined in Eq. 15. The value for the bulk is $S(\infty) = 0.46$.

The more interesting quantities, the profiles of the density fluctuations

$$\delta\rho(r) = \sqrt{\langle[\rho(r) - \langle\rho(r)\rangle]^2\rangle} \qquad (25)$$

and the orientational fluctuations

$$\delta S(r) = \sqrt{\langle[S(r) - \langle S(r)\rangle]^2\rangle} \qquad (26)$$

are shown in Fig. 9. The important result is that the density and orientational fluctuations decrease with increasing distance from the protein and settle to some constant values for the bulk $\delta\rho(\infty) = 0.04$ and $\delta S(\infty) = 0.2$, respectively. The semi-log plot in Fig. 9 of the fluctuations indicate an exponential decay according to

$$\delta S(r) - \delta S(\infty) \sim \exp(-r/\xi) \qquad (27)$$

and for the density fluctuations similarly where $\xi/\sigma_L \approx 3.2$. This is in qualitative agreement with earlier mean-field calculations (Schröder, 1977; Pearson et al., 1984) which yield

$$\delta S(r) - \delta S(\infty) \sim K_o(r/\xi) \qquad (28)$$

where $K_o(x)$ is the modified Bessel function with the limiting behavior $K_o(x) \sim \exp(-x)/\sqrt{x}$ for $x \to \infty$. Fitting the latter function to our data in Fig. 9 we get a slightly larger correlation function of $\xi/\sigma_L \approx 3.8$.

It is important to note that the profiles of the average orientational order and density are qualitatively quite distinct from their corresponding fluctuations as it can be inferred by comparing Figs. 8 and 9. Whereas the $\langle\rho(r)\rangle$ decays rapidly to $\rho(\infty)$, the corresponding fluctuation $\langle\delta\rho(r)\rangle$ is long-ranged. Therefore the latter observation together

with the distance distribution $P(r)$ (Fig. 7) indicates that the overlap of the fluctuation profiles rather than the overlap of $\langle\rho(r)\rangle$ or $\langle S(r)\rangle$ are responsible for the lipid-mediated attraction between proteins. This interpretation is somewhat different from the conclusions based on Marcelja's work (Marcelja, 1976) where the attraction is attributed to the overlap of $\langle S(r)\rangle$ rather than $\langle\delta S(r)\rangle$. Our suggestions are more in agreement with the conclusions of Schröder's work (Schröder, 1977) based on linear response theory.

It is interesting to note that the fluctuation-induced attraction, as it has been observed in the present simulations, is not of pure enthalpic origin as in previous work (Marcelja, 1976), but is due to a balance between enthalpic forces and the counteracting forces from the entropy of mixing that is included in the present Monte Carlo simulations.

Using conventional mean-field Landau theory (de Gennes, 1974) it is possible to relate the fluctuations to an effective potential between the two proteins. Starting with an expansion of the change of the total free energy density in terms of the orientational order parameter (Schröder, 1977; Pearson et al. 1984)

$$\Delta F(r) = a\phi^2(r) + b\left[\frac{\partial}{\partial r}\phi(r)\right]^2 + \ldots . \qquad (29)$$

where $\phi(r) = S(r) - S(\infty)$ and a and b are some constants depending, e.g., on temperature and material properties, one obtains an effective potential $U(r)$ between two proteins by identifying $U(r) = \Delta F(r)$ (Marcelja, 1976) and $\delta S(r) \approx \phi(r)$, which yields, using (27) and (29)

$$U(r) \sim -\exp(-2r/\xi). \qquad (30)$$

It is interesting to note that the potential $U(r)$ is of similar form as compared to the screened Coulomb potential $\sim\exp(r/\zeta)/r$. This may be of interest concerning the stability of protein aggregates where a competition between Coulomb repulsion between charges of equal sign and the attractive potential (30) may take place.

SUMMARY AND CONCLUSIONS

Using Monte Carlo simulations we have investigated the lipid-mediated attraction between two proteins embedded in a bilayer membrane. Neglecting effects due to undulations or bending of the membrane we have focused on effects related to the fluctuations of the lipid orientational order and lipid density in the vicinity of a protein. We found two types of attraction with different regimes. A depletion-induced attraction in the range $r < \sigma_L$, where σ_L is the diameter of a lipid and r is the distance between the surfaces of the two proteins, and a fluctuation-induced attraction in the range $1 < r/\sigma_L < 6$ which originates from the overlap of the gradients of density and orientational fluctuations of the lipids around each protein.

There are several possible extensions of our present investigations. It can be expected that the correlation length ξ depends on various parameters as temperature, density, and specific properties of the lipid molecules. Another interesting aspect may be related to some cooperative effects (Pearson et al., 1984) during protein aggregation based upon the fluctuation-induced attraction.

In the present simulations we have used a membrane model where effects coming from bending elasticity are suppressed. Although membrane undulations are predicted to play a significant role during protein aggregation it is conceivable that lipid-mediated attractions as discussed in the present work are equally important for the stability of clusters of helices or proteins.

Financial support of T.S. by the Commission of the European Communities (ERBFM-BICT961451) is gratefully acknowledged.

REFERENCES

Allen, M., and D. Tildesley. 1987. Computer Simulation of Liquids. Clarendon, Oxford, UK.

Aranda-Espinoza, H., A. Berman, N. Dan, P. Pincus, and S. Safran. 1996. Interaction between inclusions embedded in membranes. *Biophys. J.* 71:648–656.

Asakura, S., and F. Oosawa. 1958. Interaction between paticles suspended in solutions of macromolecules. *J. Polym. Sci.* 33:183–192.

Baumgärtner, A. 1995. Asymmetric partitioning of a polymer into a curved membrane. *J. Chem. Phys.* 103:10669–10674.

Ben-Tal, N., and B. Honig. 1996. Helix-helix interactions in lipid bilayers. *Biophys. J.* 71:3046–3050.

Bruinsma, R., M. Goulian, and P. Pincus. 1994. Self-assembly of membrane junctions. *Biophys. J.* 67:746–750.

de Gennes, P. G. 1974. The Physics of Liquid Crystals. Oxford University Press, Oxford, UK. 23–58.

Dickman, R., and A. Yethiraj. 1994. Polymer-induced forces between colloidal particles. A Monte Carlo simulation. *J. Chem. Phys.* 100: 4683–4690.

Egberts, E., S. J. Marrink, and H. J. C. Berendsen. 1994. Molecular dynamics simulation of a phospholipid membrane. *Eur. Biophys. J.* 22:423–436.

Gennis, R. B. 1989. Biomembranes: Molecular Structure and Function. Springer, New York.

Goulian, M., R. Bruinsma, and P. Pincus. 1993. Long-range forces in heterogeneous fluid membranes. *Europhys. Lett.* 22:145–150.

Gruler, H., and E. Sackmann. 1977. Long-range protein-protein interaction in membranes. *Croatica Chem. Acta.* 49:379–388.

Haas, F. M., R. Hilfer, and K. Binder. 1995. Off lattice Monte Carlo simulation of a coarse grained model for Langmuir monolayers. *J. Chem. Phys.* 102:2960–2969.

Israelachvili, J. 1992. Intermolecular and Surface Forces. 2nd Ed. Academic Press, London.

Lemmon, M. A., and D. M. Engelman. 1994. Specificity and promiscuity in membrane helix interactions. *Quart. Rev. Biophys.* 27:157–218.

Marcelja, S. 1976. Lipid-mediated protein interaction in membranes. *Biochim. Biophys. Acta* 455:1–7.

Meijer, E. J., and D. Frenkel. 1994. Colloids dispersed in polymer solutions. A computer simulation study. *J. Chem. Phys.* 100:6873–6887.

Mouritsen, O. G., and M. Bloom. 1993. Models of lipid-protein interactions in membranes. *Ann. Rev. Biophys. Biomol. Struct.* 22:145–171.

Odell, E., and G. Oster. 1994. Curvature segregation of proteins in the Golgi. *Lectures on Math. in the Life Sci.* 24:23–36.

Ohshima, Y. N., H. Sakagami, K. Okumoto, A. Tokoyoda, T. Igarashi, K. B. Shintaku, S. Toride, H. Sekino, K. Kabuto, and I. Nishio. 1997. Direct measurement of infinitesimal depletion force in a colloid-polymer mixture by laser radiation pressure. *Phys. Rev. Lett.* 78:3963–3966.

Owicki, J. C., and H. M. McConnell. 1979. Theory of protein-lipid and protein-protein interactions in bilayer membranes. *Proc. Natl. Acad. Sci. USA.* 76:4750–4754.

Pearson, T. L., J. Edelman, and S. I. Chan. 1984. Statistical mechanics of lipid membranes. Protein correlation functions and lipid ordering. *Biophys. J.* 45:863–871.

Peters, R. 1988. Lateral mobility of proteins and lipids in the red cell membrane and the activation of adenylate cyclase by β-adrenergic receptors. *FEBS Lett.* 234:1–7.

Schröder, H. 1977. Aggregation of proteins in membranes. An example of fluctuation-induced interactions in liquid-crystals. *J. Chem. Phys.* 67: 1617–1619.

Sintes, T., and A. Baumgärtner. 1997. Short-range attraction between two colloids in a lipid monolayer. *J. Chem. Phys.* 106:5744–5750.

Xiang, T-X. 1993. A computer simulation of free-volume distributions and related structural properties in a model lipid bilayer. *Biophys. J.* 65: 1108–1120.